American Mineralogist, Volume 84, pages 203–206, 1999

In situ structure determination of the high-pressure phase of Fe_3O_4

YINGWEI FEI,[1,*] DANIEL J. FROST,[1,†] HO-KWANG MAO,[1] CHARLES T. PREWITT,[1] AND DANIEL HÄUSERMANN[2]

[1]Geophysical Laboratory and Center for High Pressure Research, Carnegie Institution of Washington, 5251 Branch Road, N.W., Washington, D.C. 20015, U.S.A.
[2]European Synchrotron Radiation Facility, BP220, F38043 Grenoble Cedex, France

ABSTRACT

The crystal structure of a high-pressure Fe_3O_4 phase was determined by in situ X-ray diffraction measurements at high pressure and temperature, using an imaging plate detector and monochromatic synchrotron X-radiation. The high-pressure phase has the *Pbcm* space group ($CaMn_2O_4$-type structure) with cell parameters $a = 2.7992(3)$ Å, $b = 9.4097(15)$ Å, and $c = 9.4832(9)$ Å at 23.96 GPa and 823 K. Fe^{3+} occupies an octahedral site and Fe^{2+} is in an eightfold-coordinated site described as a bicapped trigonal prism. The high-pressure $CaMn_2O_4$-type Fe_3O_4 phase is about 6.5% more dense than the spinel form at 24 GPa.

INTRODUCTION

Magnetite (Fe_3O_4) is a mixed valence iron oxide with some Fe^{3+} ions occupying the tetrahedral sites and the Fe^{2+} and the remaining Fe^{3+} ions occupying the octahedral sites in the spinel structure (space group $Fd\bar{3}m$) (e.g., Fleet 1981). Its high-pressure behavior has been extensively studied by X-ray diffraction (Mao et al. 1974; Huang and Bassett 1986; Nakagiri et al. 1986; Finger et al. 1986; Pasternak et al. 1994), Mössbauer spectroscopy (Mao et al. 1977; Pasternak et al. 1994), and electrical resistivity measurements (Samara 1968; Ramasesha et al. 1994; Rozenberg et al. 1996; Morris and Williams 1997) because of its geophysical importance and its interesting magnetic properties at high pressure. Mao et al. (1974) demonstrated that magnetite transforms to a high-pressure phase at about 25 GPa. The X-ray diffraction pattern for the high-pressure phase, collected using a diamond cell diffraction camera (Bassett et al. 1967) and conventional X-ray source, was indexed on a monoclinic cell. Because relatively few diffraction lines were observed, the structure assignment was tentative. The high-pressure phase transition was confirmed by Huang and Bassett (1986) who determined its temperature dependence. The structural transition is also accompanied with changes in magnetic properties (Mao et al. 1977; Pasternak et al. 1994) and electrical resistivity (Morris and Williams 1997). Without knowledge of the crystal structure of the high-pressure phase, ambiguity exists in interpreting the Mössbauer spectra of Fe_3O_4 at high pressures.

X-ray diffraction data for the high-pressure phase of Fe_3O_4 collected in previous studies suffer from either low resolution or broad diffraction peaks that sometimes overlap those of magnetite due to the sluggish transition at room temperature. This study presents new diffraction data for the high-pressure phase collected on an imaging plate using monochromatic synchrotron X-ray radiation. The diffraction data contain accurate structural information with high resolution. The high quality data allow us to solve the crystal structure of the high-pressure phase of Fe_3O_4.

EXPERIMENTAL PROCEDURE

The starting material used in this study is synthetic magnetite with enriched ^{57}Fe, the same starting material used in the Mössbauer spectroscopic study by Mao et al. (1977). High-pressure–high-temperature experiments were conducted using an externally heated high-temperature diamond-anvil cell. The high-temperature cell is capable of achieving pressures greater than 125 GPa at temperatures up to 900 °C (Fei and Mao 1994; Fei 1996). A detailed description of this cell was given by Fei (1996). Here, we used 500 μm flat diamond anvils. The powdered magnetite sample was compacted in a sample chamber, 200 μm in diameter by 49 μm in thickness, drilled in a preindented rhenium gasket. A layer of NaCl powder was placed on the top of the magnetite sample to serve as a pressure-transmitting medium (especially at high temperatures) and as a pressure calibrant. A small piece (<10 μm) of thin gold foil was placed in only one quarter of the sample chamber as a pressure calibrant to obtain diffraction data with or without gold diffraction peaks. One small ruby grain (~5 μm) was also placed in the sample chamber for initial pressure determination at room temperature. At high T, sample temperature was measured by a Pt/Pt-10%Rh thermocouple placed near the sample chamber, whereas pressure was determined by measuring the lattice parameters of an internal standard (Au or NaCl), based on its P-V-T equation of state (Anderson et al. 1989; Birch 1978).

We initially compressed the sample to $P = 34.45$ GPa at room temperature, based on the ruby pressure scale (Mao et al. 1978). At this pressure, magnetite should have transformed to the high-pressure phase completely (Huang and Bassett 1986). We then took the diamond cell to the European Synchrotron Radiation Facility (ESRF) for in situ X-ray diffraction measurements. The experimental setup at ESRF (beamline ID30) was described by

*E-mail: fei@gl.ciw.edu
†Present address: Nowat Bayerisches Geoinstitut Universitaet Bayreuth, D-95440 Bayreuth, Germany.

0003-004X/99/0102–0203$05.00

Häusermann and Hanfland (1996). A monochromatic beam (Si 111 monochromator) with wavelength of 0.4253 Å was used in the experiments. The beam was focused down to a <15 μm spot by two multilayer mirrors. The diffraction data were recorded on an imaging plate and read with a scanner. The details of the imaging plate technique have been described by Amemiya (1995) and Nelmes and McMahon (1994). The sample-plate distance was 495.62 mm, determined by measuring the lattice parameter of gold at a known pressure determined from ruby fluorescence at room temperature. The two-dimensional imaging plate data were reduced to an intensity vs. 2θ plot using the FIT2D program (Hammersley et al. 1996).

Results and discussion

In situ X-ray diffraction measurements of Fe_3O_4 were made at 34.45 GPa and 300 K, 26.41 GPa and 723 K, 23.96 GPa and 823 K, and 9.04 GPa and 923 K. Figure 1 shows the pressure-temperature path of our experiments and Figure 2 shows the X-ray diffraction patterns. From the phase boundary determined by Huang and Bassett (1986), three of our experiments (Fig. 1) are within the stability field of the high-pressure phase of Fe_3O_4. The diffraction data corresponding to these conditions confirm the existence of the high-pressure phase with a rather complicated diffraction pattern (Fig. 2). The diffraction peaks at room temperature are relatively broad. With increasing temperature, the peaks sharpen because of completion of the transformation and decrease of the deviatoric stress in the sample chamber. The broad peak at $2\theta = 10^\circ$ in the 300 K pattern, indicative of the low-pressure phase magnetite, disappears at about 623 K, indicating complete conversion of magnetite to the high-pressure phase. The strongest peak at $2\theta = 9.5^\circ$ was assigned as a single peak in the early study by Mao et al. (1974) but in fact is a triplet as evident in the diffraction patterns at 823 K and 23.96 GPa (Fig. 2). At 923 K, the sample pressure was decreased to 9.04 GPa, and the observed diffraction pattern was indexed on a cubic cell of magnetite (Fig. 2). The refined unit-cell parameters at 923 K and 9.04 GPa for magnetite and NaCl (B1 structure) are 8.3348(1) Å and 5.2954(2) Å, respectively. The transformation from the high-pressure phase to magnetite with decreasing pressure at high temperature (Fig. 1) is consistent with the phase boundary determined by Huang and Bassett (1986). The high-pressure Fe_3O_4 phase is non-quenchable, and its structure can be determined only by in situ X-ray diffraction measurements at high pressure and temperature.

The imaging plate data collected at ESRF are of high resolution and contain accurate intensity information. Its resolution is comparable to that of a conventional powder diffractometer, $\Delta d/d$ of 0.001 at 2 Å, and about an order of magnitude higher than that of energy-dispersive technique, $\Delta d/d$ of 0.01 at 2 Å. High angular resolution can be further achieved by increasing the sample-plate distance. The high-quality data are good enough for Rietveld structure refinement, providing the space group of the phase is known (Hammersley et al. 1996). The observed diffraction data for the high-pressure phase of Fe_3O_4 cannot be indexed with the monoclinic cell proposed by Mao et al. (1974). Using systematics of high-pressure post-spinel transformations in materials such as $MgAl_2O_4$ (Irifune et al. 1991) and $CaAl_2O_4$ (Reid and Ringwood 1969), we initially tried to index the observed pattern on an orthorhombic cell of the $CaFe_2O_4$-type structure. All the observed d-spacings can indeed be explained by an orthorhombic cell, but the observed intensities are not consistent with the space group *Pnam* ($CaFe_2O_4$-type structure). Further structure refinements indicate that the high-pressure phase of Fe_3O_4 has the space group *Pbcm* ($CaMn_2O_4$-type structure) with cell parameters, $a = 2.799?(3)$ Å, $b = 9.4097(15)$ Å, and $c = 9.4832(9)$ Å. Figure 3 shows the Rietveld

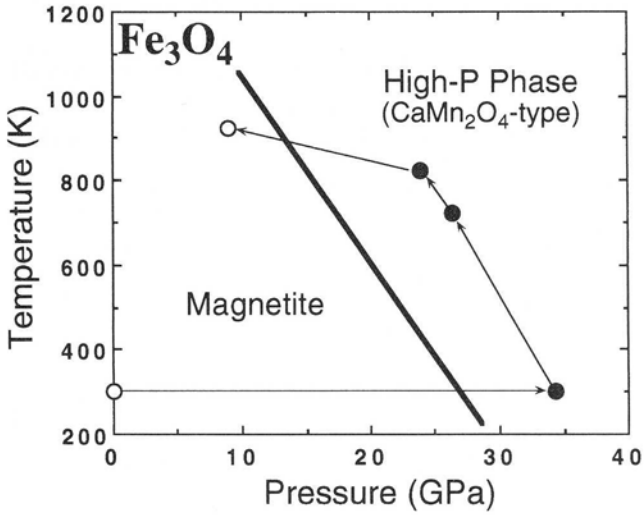

Figure 1. Phase transformation in Fe_3O_4 at high pressures and temperatures. The solid and open circles indicate P-T conditions under which the high-pressure Fe_3O_4 phase and magnetite were observed, respectively. The arrows indicate the experimental P-T path. Thick line represents the phase boundary of the transformation from magnetite to its high-pressure phase, determined by Huang and Bassett (1986).

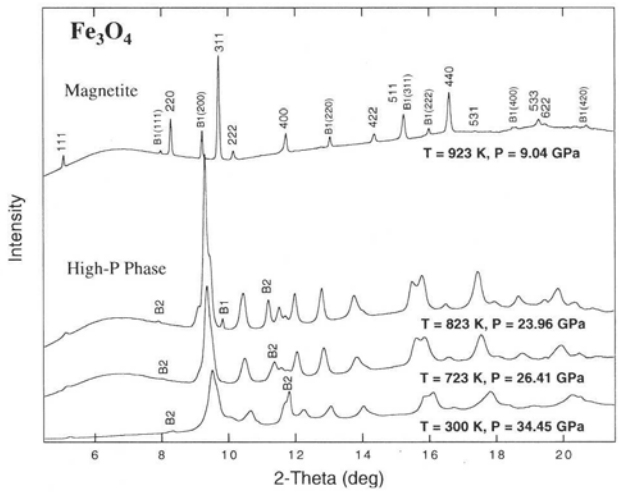

Figure 2. Representative X-ray diffraction patterns collected at 34.45 GPa and 300 K, 26.41 GPa and 723 K, 23.96 GPa and 823 K, and 9.04 GPa and 923 K, with wavelength of 0.4253 Å. The diffraction pattern at 9.04 GPa and 923 K was indexed on a cubic cell of magnetite. The *hkl* indices are indicated for each diffraction peak and indices for NaCl (B1 structure) are also shown. The diffraction patterns at 300, 723, and 823 K are from the high-pressure Fe_3O_4 phase and the diffraction peaks of NaCl are marked by B2 and B1.

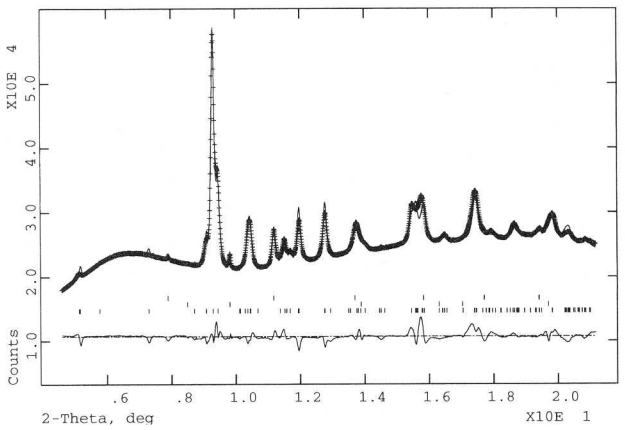

FIGURE 3. Observed (crosses) and calculated (solid line) X-ray diffraction pattern for the orthorhombic high-pressure phase of Fe_3O_4 at 23.96 GPa and 823 K. The experimental data were collected with wavelength of 0.4253 Å. Tick marks for NaCl (B2), NaCl (B1), and the high-pressure Fe_3O_4 phase are shown in decending order below the pattern. The difference curve is shown at the bottom. The refinement is based on the space group Pbcm with cell parameters, a = 2.7992(3) Å, b = 9.4097(15) Å, and c = 9.4832(9) Å.

TABLE 1. Refined unit-cell and atomic positional parameters and selected interatomic distances (Å) for the high-pressure phase of Fe_3O_4 at 23.96 GPa and 823 K.

Atom	Index	*x*	*y*	*z*
Fe^{2+}	4d	0.724(6)	0.3757(5)	0.25
Fe^{3+}	8e	0.246(4)	0.1107(4)	0.0879(4)
O^{2-}	4c	0.506(5)	0.25	0
O^{2-}	4d	0.180(9)	0.2447(19)	0.25
O^{2-}	8e	0.296(11)	0.4899(13)	0.0980(15)

Bond distances

Fe^{2+}—O2	1.775(12) ×1	Fe^{3+}—O1	1.715(12) ×1
Fe^{2+}—O2	1.959(14) ×1	Fe^{3+}—O3	1.716(25) ×1
Fe^{2+}—O3	2.159(25) ×2	Fe^{3+}—O3	1.899(29) ×1
Fe^{2+}—O3	2.409(21) ×2	Fe^{3+}—O2	1.997(5) ×1
Fe^{2+}—O1	2.718(12) ×2	Fe^{3+}—O3	2.006(14) ×1
Fe^{2+}— Fe^{2+}	2.7992(3)	Fe^{3+}—O1	2.589(12) ×1
Fe^{3+}— Fe^{3+}	2.7992(3)		
Fe^{2+}— Fe^{3+}	2.695(5)		

Notes: The final discrepancy indices (Larson and Von Dreele 1986) are R_{wp} = 0.019, R_p = 0.013, $R(F^2)$ = 0.17, and reduced $\chi 2$ = 9.4. Space group: *Pbcm*; *Z* = 4, *a* = 2.7992(3) Å, *b* = 9.4097(15) Å, and *c* = 9.4832(9) Å.

refinement results for the orthorhombic high-pressure phase of Fe_3O_4, using the program package GSAS (Larson and Von Dreele 1986). Both B1 and B2 structures of NaCl were observed at this pressure-temperature condition. The refined unit-cell parameters for B1 and B2 are 4.9696(9) Å and 3.0879(8) Å, respectively. The structure refinement parameters for the high-pressure phase of Fe_3O_4 are listed in Table 1. The refinement yielded a good agreement between the observed and calculated X-ray diffraction patterns.

The $CaMn_2O_4$-type structure, closely related to the $CaFe_2O_4$-type structure and a distortion of the more symmetrical $CaTi_2O_4$-type, is one of the densest AB_2O_4 structures. The trivalent ions occupy the octahedral sites while the divalent ions occupy the eightfold-coordinated site. Reid and Ringwood (1969) observed that Mn_3O_4 and $CaAl_2O_4$ transform to the $CaMn_2O_4$-type and the $CaFe_2O_4$-type structure, respectively, at about 10 GPa. Recent high-pressure experiments showed that $MgAl_2O_4$ spinel also transforms to the $CaFe_2O_4$-type structure at about 25 GPa (Irifune et al. 1991). It is not surprising that Fe_3O_4 takes the $CaMn_2O_4$-type structure at high pressure, forming a dense high-pressure phase. The high-pressure $CaMn_2O_4$-type Fe_3O_4 is about 6.5% more dense than the spinel form at 24 GPa. The structure refinements indicated that the octahedral and the eightfold-coordinated sites, occupied by the Fe^{3+} and the Fe^{2+} ions, respectively, are rather distorted. The Fe^{3+}-O^{2-} bond lengths for the octahedral sites and the Fe^{2+}-O^{2-} bond lengths for the eightfold-coordinated sites at 24 GPa range from 1.715 to 2.589 Å and from 1.775 to 2.719 Å, respectively (Table 1). The average Fe^{3+}-O^{2-} bond length for the sixfold-coordinated site at 24 GPa is about 1.99 Å, slightly smaller than the 1-atm value of 2.06 Å because of the pressure effect. The shortest Fe^{2+}-O^{2-} bond length for the eightfold-coordinated site is about 1.775 Å, which appears to be unusually small. However, the average Fe^{2+}-O^{2-} bond length (2.288 Å) is consistent with the expected value for the eightfold-coordinated site at high pressure (cf. the value of 2.310 Å at 1 atm). Increasing the shortest Fe^{2+}-O^{2-} bond length to 1.98 Å would lead to the average bond length of 2.378 Å, unreasonably larger than the 1-atm value for the eightfold-coordinated site.

The structure determination of the high-pressure Fe_3O_4 phase will allow us to understand the magnetic and electrical properties of Fe_3O_4 at high pressures. The observed two quadrupole doublets for the high-pressure Fe_3O_4 phase by Mössbauer measurements (Mao et al. 1977; Pasternak et al. 1994) are consistent with the current structure assignment in which the Fe^{3+} and the Fe^{2+} ions occupy two distinct crystallographic sites. The orthorhombic high-pressure phase is not magnetically ordered on the basis of Mössbauer measurements (Mao et al. 1977; Pasternak et al. 1994) whereas magnetite is the best known example of ferrimagnetic materials. The electrical resistivity measurements of Fe_3O_4 at high pressures (Morris and Williams 1997) showed that the high-pressure phase is not metallic, consistent with the atomic bond distances determined here. Thus the magnetic transition in Fe_3O_4, corresponding with the structural transformation, is best described by the change from the ferrimagnetic to the paramegnetic state (Mao et al. 1977).

ACKNOWLEDGMENTS

This research was supported by the National Science Foundation Center for High Pressure Research and the Carnegie Institution of Washington. We acknowledge ESRF for providing us with beam time. We thank L.W. Finger for helpful discussions, W.A. Bassett and R.T. Downs for useful comments, and M. Kunz for experiment assistance.

REFERENCES CITED

Amemiya, Y. (1995) Imaging plate for use with synchrotron radiation. Journal of Synchrotron Radiation, 2, 13–22.

Anderson, O.L., Isaak, D.G., and Yamamoto, S. (1989) Anharmonicity and the equation of state for gold. Journal of Applied Physics, 65, 1534–1543.

Bassett, W.A., Takahashi, T., and Stook, P.W. (1967) X-ray diffraction and optical observations on cristalline solids up to 300 kolobars. Review of Scientific Instruments, 38, 37–42.

Birch, F. (1978) Finite strain isotherm and velocities for single-crystal and polycrystalline NaCl at high pressures and 300 K. Journal of Geophysical Research, 83, 1257–1268.

Fei, Y. (1996) Crystal chemistry of FeO at high pressure and temperature. In M.D. Dyar, C. McCammon, and M.W. Shaefer, Eds., Mineral Spectroscopy: A Tribute to Roger

G. Burns, p. 243–254. Special Publication no. 5. The Geochemical Society, Houston.

Fei, Y. and Mao, H.K. (1994) In situ determination of the NiAs phase of FeO at high pressure and temperature. Science, 266, 1668–1680.

Finger, L.W., Hazen, R.M., and Hofmeister, A.M. (1986) High-pressure crystal chemistry of spinel ($MgAl_2O_4$) and magnetite (Fe_3O_4): Comparisons with silicate spinels. Physics and Chemistry of Minerals, 13, 215–220.

Fleet, M.E. (1981) The structure of magnetite. Acta Crystallographica, B37, 917–920.

Hammersley, A.P., Svensson, S.O., Hanfland, M., Fitch, A.N., and Häusermann, D. (1996) Two-dimensional detector software: From real detector to idealised image or two-theta scan. High Pressure Research, 14, 235–248.

Häusermann, D. and Hanfland, M. (1996) Optics and beamlines for high-pressure research at the European Synchrotron Radiation Facility. High Pressure Research, 14, 223–234.

Huang, E. and Bassett, W.A. (1986) Rapid determination of Fe_3O_4 phase diagram by synchrotron radiation. Journal of Geophysical Research, 91, 4697–4703.

Irifune, T., Fujino, K., and Ohtani, E. (1991) A new high-pressure form of $MgAl_2O_4$. Nature, 349, 409–411.

Larson, A.C. and Von Dreele, R.B. (1986) GSAS manual, Report LAUR 86-748, Los Alamos National Laboratory.

Mao, H.K., Takahashi, T., Bassett, W.A., Kinsland, G.L., and Merrill, L. (1974) Isothermal compression of magnetite to 320 kbar and pressure-induced phase transformation, Journal of Geophysical Research, 79, 1165–1170.

Mao, H.K., Virgo, D., and Bell, P.M. (1977) High-pressure 57Fe Mössbauer data on the phase and magnetic transitions of magnesioferrite ($MgFe_2O_4$), magnetite (Fe_3O_4), and hematite (Fe_2O_3). Carnegie Institution of Washington YearBook, 76, 522–525.

Mao, H.K., Bell, P.M., Shaner, J.W., and Steinberg, D.J. (1978) Specific volume measurements of Cu, Mo, Pd, and Ag and calibration of the ruby R_1 fluorescence pressure gauge from 0.06 to 1 Mbar. Journal of Applied Physics, 49, 3276–3283.

Morris, E.R. and Williams, Q. (1997) Electrical resistivity of Fe_3O_4 to 48 GPa: Compression-induced changes in electron hopping at mantle pressures. Journal of Geophysical Research, 102, 18139–18148.

Nakagiri, N., Manghnani, M.H., Ming, L.C., and Kimura, S. (1986) Crystal structure of magnetite under pressure. Physics and Chemistry of Minerals, 13, 238–244.

Nelmes, R.J. and McMahon, M.I. (1994) High-pressure powder diffraction on synchrotron sources. Journal of Synchrotron Radiation, 1, 69–80.

Pasternak, M.P., Nasu, S., Wada, K., and Endo, S. (1994) High-pressure of magnetite. Physical Review, B50, 6446–6449.

Ramasesha, S.K., Mohan, M., Singh, A.K., Honig, J.M., and Rao, C.N.R. (1994) High-pressure study of Fe_3O_4 through the Verwey transition. Physical Review, B50, 13789–13791.

Reid, A.F. and Ringwood, A.E. (1969) Newly observed high pressure transformations in Mn_3O_4, $CaAl_2O_4$, and $ZrSiO_4$. Earth and Planetary Science Letters, 6, 205–208.

Rozenberg, G.K., Hearne, G.R., Pasternak, M.P., Metcalf, P.A., and Honig, J.M. (1996) Nature of the Verwey transition in magnetite (Fe_3O_4) to pressures of 16 GPa. Physical Review, B53, 6482–6487.

Samara, G.A. (1968) Effect of pressure on the metal-nonmetal transition and conductivity of Fe_3O_4. Physical Review Letters, 21, 795–797.

MANUSCRIPT RECEIVED AUGUST 7, 1998
MANUSCRIPT ACCEPTED OCTOBER 2, 1998
PAPER HANDLED BY JAMES W. DOWNS